ISSN 2070-0482, Mathematical Models and Computer Simulations, 2023, Vol. 15, No. 2, pp. 210–226. © Pleiades Publishing, Ltd., 2023.
Russian Text © The Author(s), 2022, published in Matematicheskoe Modelirovanie, 2022, Vol. 34, No. 8, pp. 73–96.

Numerical Simulation of Dynamic Processes in a Medium of Fine-Grained Solid Particles

M. Y. Nemtsev[a,b,*], I. S. Menshov[a,b], and I. V. Semenov[a]

[a] *Scientific Research Institute of System Analysis, Russian Academy of Sciences, Moscow, Russia*

[b] *Keldysh Institute of Applied Mathematics, Russian Academy of Sciences, Moscow, Russia*

**e-mail: nemtsev@niisi.ras.ru*

Received May 17, 22; revised June 14, 2022; accepted June 27, 2022

Abstract—A simplified model system of governing equations describing the motion of an ensemble of solid fine-grained particles arising in the continual description of two-phase dispersed media is considered. The specific features of this system consist of a discontinuity in the characteristic velocity of the propagation of small disturbances when the volume fraction equals the value of dense packing and the possibility of forming void regions free of particles. A modification to the Godunov method based on the exact solution to the Riemann problem and an approximate Harten–Lax–van Leer (HLL)-type solver, which takes into account the mentioned specific features, is proposed for the system considered. The methods developed are verified on a set of test problems that are analogs of the benchmarks by Sod and Shu–Osher, which are well-known in gas dynamics. The problem of decompaction of a side-wall layer of compressed particles is also considered. The mechanism of particle detachment and development of a near-wall void zone free of particles is described. The numerical results are compared with the available analytical data.

Keywords: two-phase dispersed media, continuum model of ensemble of solid particles, Riemann problem, Godunov method

DOI: 10.1134/S2070048223020138

1. INTRODUCTION

Multiphase flows of dispersed mixtures in the case when the volume fraction of the dispersed phase varies over a wide range—from the values of rarefied practically noninteracting particles to the values of close packing—occur in many applied problems, for example, in the study of internal ballistic processes [1, 2], dispersion of dust layers behind shock waves [3], detonation propagation in dispersed systems [4], and other. The model of two interpenetrating continuums is usually used as the main mathematical model for describing such processes. In this model, each phase is described by its own continuum and characterized by its own fields of density, velocity, pressure, and other flow parameters. The system of constitutive equations is derived based on the laws of conservation of mass, momentum, and energy for each phase and a certain model of force and thermal interaction between phases.

For the case when both phases are compressible media with a spherical stress tensor and the corresponding thermodynamic equations of state, the continuum model of a two-phase dispersed mixture was derived quite strictly from the fundamental principles of thermodynamics in [4]. It is well known in the modern literature as the nonequilibrium Bayer–Nunziato model. Alternative continuum models for the flow of two-phase dispersed mixtures in regimes corresponding to small values of the volume fraction of the dispersed component were also considered in [5, 6]. The construction of a model and analysis of the properties of thermodynamic consistency and hyperbolicity for the cases of a small volume fraction of the dispersed phase (rarefied mixture) and a relatively large one, corresponding to a dense packing of particles of the dispersed phase, are given in [7–9]. In these papers, the assumption that both phases are compressible is used significantly.

Relatively few works are available on models for the case of an incompressible solid dispersed phase. First of all, the works of A.N. Kraiko with colleagues should be noted. The construction of a two-phase two-velocity continuum model under the assumption that there are no collisions of particles is considered in [5, 10]. The questions of the correctness of the Cauchy problem that arise in this case are studied in [11,

12]. The works [13, 14] study dusty gas and the two-phase boundary layer. The mathematical features of systems of Euler equations without pressure are discussed in [15, 16].

In this paper, some issues are studied related to numerical simulation of the flow of a two-phase dispersed medium, which is a nonequilibrium mixture of the gas carrier component and solid, small, incompressible, and indeformable particles. The application of the model of interpenetrating continuums for this case was considered in [1, 5]. To describe regimes with a dense packing of particles of the dispersed phase, an additional tensor of intergranular interaction is introduced in these works. Its spherical part is responsible for the intergranular pressure, which occurs only when the volume fraction is greater than a certain critical value. It corresponds to the value of the close packing of the particles. At lower values of the volume fraction, the intergranular pressure disappears.

The system of constitutive equations of the full model, without taking into account the terms describing the interfacial force and thermal interaction, consists of equations describing the motion of the gas phase

$$\begin{cases} \dfrac{\partial(\alpha\rho)}{\partial t} + \nabla^k(\alpha\rho u_k) = 0, \\ \dfrac{\partial(\alpha\rho\mathbf{u})}{\partial t} + \nabla^k(\alpha\rho\mathbf{u}u_k) = -\alpha\nabla p, \\ \dfrac{\partial(\alpha\rho(e+0.5u^2))}{\partial t} + \nabla^k(\alpha\rho(e+0.5u^2)u_k) = -\nabla^k(\alpha p u_k) - p\nabla^k(\beta v_k) \end{cases} \tag{1}$$

and a system of equations describing the dynamics of the dispersed phase

$$\begin{cases} \dfrac{\partial(\beta\delta)}{\partial t} + \nabla^k(\beta\delta v_k) = 0, \\ \dfrac{\partial(\beta\delta\mathbf{v})}{\partial t} + \nabla^k(\beta\delta\mathbf{v}v_k) = -\beta\nabla p + \nabla(\beta\sigma), \\ \dfrac{\partial(\beta\delta(\varepsilon+0.5v^2+B_c))}{\partial t} + \nabla^k(\beta\delta(\varepsilon+0.5v^2+B_c)v_k) = \nabla^k(\beta\sigma_{ik}v_i) - \beta v_k\nabla^k p. \end{cases} \tag{2}$$

The following notation is introduced here: α and β are the volume fractions of the carrier gas and dispersed phases, ρ and δ are density, $\mathbf{u}$ and $\mathbf{v}$ are speed, e and ε are the internal energies of the gas and particles, respectively, p is the pressure in the gas, $B_c = B_c(\beta)$ is the configuration energy of particles, and σ_{ik} is the interparticle interaction tensor. The spherical part of tensor σ is the intergranular pressure. The total energy of the dispersed phase is the sum of the thermal part of the energy $\varepsilon = \varepsilon(T_p)$ determined by the particle temperature T_p, kinetic energy, and configurational energy (densification energy), determined by the volume fraction and related to the intergranular pressure σ, $\sigma = \beta\delta\left(dB_c/d\beta\right)$ [17].

Equations (1) and (2) are used in [18, 19] to describe the processes of propagation and damping of shock waves in a medium with densely packed solid particles. In these works and in [20, 21], some issues related to the peculiarities of the numerical solution of nonconservative systems of equations of two-phase hydrodynamics are discussed. In [22], a method for the approximate solution of the Riemann problem for an arbitrary nonconservative system of hyperbolic equations is proposed, which takes into account the complete set of eigenvalues of the Jacobi matrix and the complete wave configuration of the problem corresponding to this set.

One of the features of the model considered is related to the degeneration of the intergranular pressure when the volume fraction of particles falls below the value corresponding to their close packing. In other words, the intergranular pressure becomes zero at values of the volume fraction less than some critical value. This leads, firstly, to a discontinuity in the propagation velocity of small disturbances in the dispersed phase and, secondly, to the possibility of the formation of particle-free regions. These factors must be taken into account when developing a numerical method. The numerical method must reproduce all the main physical features of dynamic processes in the dispersed phase, including the discontinuity and the formation of void regions in the particle phase. To this end, let us consider a simplified model that describes the motion of only the dispersed (condensed) phase without taking into account the gas phase and try to develop a numerical method for it, taking into account the features of the model mentioned above.

The model simplified system of equations, which will be presented in this paper, can be considered as a model for describing the dynamics of the dispersed phase of particles, neglecting the effect of the carrier

phase (in a vacuum). In addition, this system arises in the numerical solution of the complete system of two-phase equations by the method of decoupling into physical processes.

In the following sections, an analysis of a simplified continuum model of the motion of an ensemble of particles is given, an exact solution of the Riemann problem and a two-wave approximate solution similar to the Harten–Lax–van Leer (HLL) approximation for gas dynamics, are considered [23]. The solutions are used to construct a numerical method of the Godunov type of the second order of accuracy, which takes into account the indicated features of the model. The method is verified and tested on a set of one-dimensional problems related to the formation of wave structures of the compaction and decompression of particles during shock-wave interactions.

2. SYSTEM OF DEFINING EQUATIONS AND ITS PROPERTIES

We consider a simplified mathematical model that describes the dynamics of an ensemble of solid nondeformable particles in a vacuum in the continuum approximation. It is represented by the system of equations (2) in which all terms related to the carrier gas phase are neglected. In addition, we also neglect the deviatoric part of the intergranular interaction tensor and take into account only its spherical part, the intergranular pressure. The energy equation of the dispersed phase is also not taken into account, since in the considered approximation it does not affect the first two equations (2) and determines the thermodynamic state of particles (temperature). For simplicity, we also restrict ourselves to the one-dimensional approximation. Then the system of defining equations can be written as follows:

$$\begin{cases} \dfrac{\partial \beta}{\partial t} + \dfrac{\partial \beta u}{\partial x} = 0, \\ \dfrac{\partial \beta u}{\partial t} + \dfrac{\partial (\beta u^2 + \beta \sigma)}{\partial x} = 0. \end{cases} \tag{3}$$

The type of dependence of the intergranular pressure is determined both by the shape and the physical properties of a certain particle material [1, 17]. In the case under consideration, in view of the assumption of the incompressibility of the dispersed phase, the process of particle compaction leads only to an increase in their volume fraction. Intergranular pressure is introduced to limit the growth of the volume fraction of particles. It is determined by the following empirical dependence on the volume fraction:

$$\sigma(\beta) = \begin{cases} \dfrac{B}{\delta}\left[\left(\dfrac{1-\beta_*}{1-\beta}\right)^k - 1\right], & \beta \geq \beta_* \\ 0, & \beta < \beta_*. \end{cases} \tag{4}$$

Here the parameter β_* determines the critical volume fraction of particles in the case of point contact. The empirical constants B and k are selected according to the experimental data on loading specimens with particle filling.

The defining system of equations in primitive variables in a nonconservative form can be written as

$$\begin{cases} \dfrac{\partial \beta}{\partial t} + u\dfrac{\partial \beta}{\partial x} + \beta \dfrac{\partial u}{\partial x} = 0, \\ \dfrac{\partial u}{\partial t} + \dfrac{c^2}{\beta}\dfrac{\partial \beta}{\partial x} + u\dfrac{\partial u}{\partial x} = 0. \end{cases} \tag{5}$$

It can be rewritten in vector form as

$$\frac{\partial \mathbf{z}}{\partial t} + \mathbf{A}\frac{\partial \mathbf{z}}{\partial x} = 0, \tag{6}$$

where $\mathbf{z} = (\beta, u)$, and

$$\mathbf{A} = \begin{Vmatrix} u & \beta \\ c^2/\beta & u \end{Vmatrix}. \tag{7}$$

The matrix of the system of equations (6) has two eigenvalues:

$$\xi = u \pm c, \tag{8}$$

where $c^2 = \partial(\beta\sigma)/\partial\beta$ and can be interpreted as the square of the propagation velocity of weak discontinuities. When approximating the intergranular pressure in form (4), we have

$$c = \sqrt{\sigma(1 + \beta k/(1-\beta)) + \beta Bk/\delta(1-\beta)}. \tag{9}$$

The system of equations (6) is not strictly hyperbolic. At a nonzero intergranular pressure, there are two different eigenvalues. When the intergranular pressure degenerates, the system has one double eigenvalue.

The model under consideration admits discontinuous solutions. Relations at a strong discontinuity bind the values of velocity and the volume fraction to the left and right of the discontinuity. They are derived from the conservative system of equations (3) and have the following form:

$$\begin{cases} \beta u - \beta_0 u_0 = D(\beta - \beta_0), \\ \beta u^2 + \beta\sigma - \beta u_0^2 - \beta_0\sigma_0 = D(\beta u - \beta_0 u_0), \end{cases} \tag{10}$$

where D is the propagation velocity of a strong discontinuity and the parameters with index 0 are related to the undisturbed region.

3. NUMERICAL METHOD

We write the conservative system of equations (3) in vector form by introducing the vector of conservative variables $\mathbf{q} = (\beta, \beta u)$ and the flow vector $\mathbf{F} = (\beta u, \beta u^2 + \beta\sigma)$. Spatial discretization of the equations is carried out on a grid with a variable step h_i. We use integer subscripts i to denote discrete values related to cells and half-integer indices $i + 1/2$ to denote the parameters at grid nodes, respectively. Applying the finite volume method, we arrive at the following semidiscrete system of equations

$$\frac{\partial \mathbf{q}_i}{\partial t} = -\frac{1}{h_i}\left[\mathbf{F}_{i+1/2} - \mathbf{F}_{i-1/2}\right], \tag{11}$$

where $\mathbf{q}_i = 1\backslash h_i \int \mathbf{C}_i \mathbf{q} dx$ is the cell's average value of the conservative vector. The numerical flow vector $\mathbf{F}_{i+1/2}$ is a function of the cell's primitive vector values interpolated into the node points $\mathbf{z}_i$, $\mathbf{F}_{i+1/2} = \mathbf{\Phi}(\mathbf{z}_i^+, \mathbf{z}_{i+1}^-)$. Here the superscripts $-$ and $+$ denote the value to the left and right of the node, respectively. The numerical flow approximation function $\mathbf{F}$ is selected according to the method of Godunov based on the solution of the Riemann problem of the decay of an arbitrary discontinuity.

To increase the order of approximation of scheme (11) in space, a subgrid reconstruction of the solution is used. To reconstruct the solution in the ith cell the values in three adjacent cells with indices $i - 1$, i, and $i + 1$ are considered. In this case, quadratic interpolation is carried out, which gives the values of the solution at the nodal points. The reconstruction procedure is described in [24] and was generalized to the case of a nonuniform grid:

$$\begin{gathered} \mathbf{z}^{\pm} = \mathbf{z} \pm 0.5 s \delta^{\pm}\left[(1 - sk^{\pm})\mathbf{\Delta}^{\mp} + (1 + sk^{\pm})\mathbf{\Delta}^{\pm}\right], \\ \mathbf{\Delta}^{+} = \mathbf{z}_{i+1} - \mathbf{z}_i, \quad \mathbf{\Delta}^{-} = \mathbf{z}_i - \mathbf{z}_{i-1}, \\ \delta^{+} = \frac{h_i}{h_i + h_{i+1}}, \quad \delta^{-} = \frac{h_i}{h_i + h_{i-1}}, \end{gathered} \tag{12}$$

where $k(\delta) = (12\delta^2 - 1)/12\delta$ is the function that determines the order of the interpolation scheme. On a uniform grid, parameter k is constant; the selection of $k = -1$ leads to the standard second-order MUSCL scheme, $k = 1$ corresponds to an unstable second-order central difference scheme, $k = 0$ corresponds to Fromm's scheme, and when $k = 1/3$, the scheme becomes a scheme of the third order of approximation [24]. At the same time, $s = \max(0, 2\Delta^+\Delta^-/(\Delta^+\Delta^+ + \Delta^-\Delta^- + \varepsilon))$ in (12), which corresponds to the Van Albada limiter [25]. The selection of the coefficient of k shown above is a generalization of the MUSCL scheme with $k = 1/3$ in the case of a nonuniform grid.

For integration over time, we use an approach of the predictor-corrector type [26]. At the first stage, the values are approximated to the cell interfaces according to (12). The obtained values $\mathbf{z}_i^+$ and $\mathbf{z}_i^-$ are used to calculate the predictor in the form

$$\tilde{\mathbf{q}}_i = \mathbf{q}_i^n - \Delta t/h_i\,[\mathbf{F}(\mathbf{z}_i^+) - \mathbf{F}(\mathbf{z}_i^-)], \tag{13}$$

where Δt is the time step.

At the second stage, the obtained predictor values are used to calculate the intermediate values of the variables

$$\mathbf{z}_i^{n+1/2} = (\tilde{\mathbf{z}}_i + \mathbf{z}_i^n)/2. \tag{14}$$

Then they are approximated to the cell interfaces using the values of the increments from the nth time step

$$\mathbf{z}_{i,n+1/2}^{\pm} = \mathbf{z}_i^{n+1/2} + (\mathbf{z}_i^{\pm} - \mathbf{z}_i). \tag{15}$$

At the final stage, the flow vectors are calculated

$$\mathbf{F}_{i+1/2} = \mathbf{\Phi}(\mathbf{z}_{i,n+1/2}^+, \mathbf{z}_{i+1,n+1/2}^-). \tag{16}$$

The described scheme is an explicit two-stage scheme. It is stable under the Courant condition, which in this case writes as follows

$$\Delta t \le (h_i/(|u_i| + c_i)) \quad \text{for all } i. \tag{17}$$

4. NUMERICAL FLOW APPROXIMATION

To select the numerical flow approximation function $\mathbf{\Phi}$, we apply Godunov's method, which suggests to approximate the numerical flow based on the solution of the Riemann problem of the decay of an arbitrary discontinuity at each node.

The Riemann problem is reduced to solving the Cauchy problem for the system of defining equations

$$\partial\mathbf{q}/\partial t + \partial\mathbf{F}/\partial x = 0 \tag{18}$$

with piecewise constant initial data

$$\mathbf{q}(0,x) = \begin{cases} \mathbf{q}_L, & \text{at} \quad x < 0, \\ \mathbf{q}_R, & \text{at} \quad x > 0. \end{cases} \tag{19}$$

The solution of the Riemann problem is self-similar and depends on the self-similar variable x/t. This condition is satisfied by the solutions of only two classes. One class consists of discontinuous solutions that describe compaction waves, crossing which results in instant change of the volume fraction and particle velocity. Exclusion of the velocity D from the relations on the strong discontinuity (10) results in the following dependence of the particle velocity on the volume fraction behind the wave front:

$$u - u_0 = \pm\sqrt{(\beta - \beta_0)(\sigma\beta - \sigma_0\beta_0)/(\beta\beta_0)} \quad \text{for } \beta \ge \beta_0, \tag{20}$$

where subscript 0 denotes the background values (before the wave front), respectively, $\sigma_0 = \sigma(\beta_0, \delta)$; i.e., it does not match index L in formula (19). Expression (20) with the "+" sign corresponds to the wave which is called the right wave. It has a mass flow $\dot{m} = \beta(u - D) = \beta_0(u_0 - D)$ less than zero, so that particles with undisturbed parameters (β_0, u_0) cross the discontinuity from right to left. Accordingly, the "–" sign is taken for the left wave, for which the mass flow rate is greater than zero, and particles with parameters (β_0, u_0) cross the discontinuity from left to right.

Strong discontinuity relations (20) are considered only for values $\beta \ge \beta_0$. The branch $\beta < \beta_0$, in principle, also takes place. It corresponds to a "decompaction shock." However, this branch must be discarded, since it corresponds to solutions that are unstable to small disturbances, which was shown by Lax in the general case of an arbitrary hyperbolic system of equations in the form of a conservation law [27].

Another class of solutions describes a centered decompaction wave, in which the flow parameters change continuously depending on the self-similar variable, $u = u(\lambda)$ and $\beta = \beta(\lambda)$. Relationships in the

decompaction wave are written as a functional dependence of the velocity on the volume fraction for values $\beta \le \beta_0$, which has the following form:

$$u = u_0 \pm \int_{\beta_0}^{\max(\beta,\beta_*)} \frac{c(\beta)d\beta}{\beta} \quad \text{for } \beta \le \beta_0, \qquad u \pm c = \lambda = x/t, \tag{21}$$

where the upper sign corresponds to the right wave with $\lambda = u + c$, and the bottom sign corresponds to the left wave with $\lambda = u - c$. For the right wave, the undisturbed region with parameters (β_0, u_0) is located to the right of the wave; and for the left wave, to the left of the wave. From the differential relations of a centered wave $\lambda\beta' - (u\beta)' = 0$, where the prime denotes the derivative with respect to λ, it can be shown that for the right wave, $\beta' > 0$, and for the left wave $\beta' < 0$ always. Therefore, in relation (21), only the branch $\beta \le \beta_0$ is considered.

Thus, taking into account the above, when passing through the right wave, the velocity is a function of the volume fraction,

$$u = u(\beta, \beta_0, u_0) = \begin{cases} u_0 + \sqrt{\dfrac{(\beta - \beta_0)(\sigma\beta - \sigma_0\beta_0)}{\beta\beta_0}} & \text{for } \beta \ge \beta_0, \\ u_0 + \displaystyle\int_{\beta_0}^{\max(\beta,\beta_*)} \frac{c(\beta)d\beta}{\beta} & \text{for } \beta < \beta_0, \end{cases} \tag{22}$$

and when passing through the left wave,

$$u = u(\beta, \beta_0, u_0) = \begin{cases} u_0 - \sqrt{\dfrac{(\beta - \beta_0)(\sigma\beta - \sigma_0\beta_0)}{\beta\beta_0}} & \text{for } \beta \ge \beta_0, \\ u_0 - \displaystyle\int_{\beta_0}^{\max(\beta,\beta_*)} \frac{c(\beta)d\beta}{\beta} & \text{for } \beta < \beta_0. \end{cases} \tag{23}$$

The calculation of the integral on the right side of (21) leads to rather cumbersome formulas. Therefore, we can consider a simple quadratic approximation for the speed of sound, which will significantly simplify the subsequent reasoning.

Assume $\overline{\beta}$ is some fixed supercritical value of the volume fraction, $\overline{\beta} > \beta_*$. We denote $\overline{c} = c(\overline{\beta})$, $c_* = c(\beta_*)$, $c'_* = c'(\beta_*)$. Then the quadratic approximation of the characteristic velocity $c = \tilde{c}(\beta)$ on the interval $[\beta_*, \overline{\beta}]$ has the following form:

$$\tilde{c}(\beta) = A\beta^2 + B\beta + C, \quad \beta \in [\beta_*, \overline{\beta}], \tag{24}$$

where the coefficients are determined from the conjugation condition $\tilde{c}(\beta_*) = c_*$, $\tilde{c}(\overline{\beta}) = \overline{c}$, and $\tilde{c}(\beta_*) = c'_*$ in the following way:

$$A = \frac{-c_* + c'_*\beta_* - c'_*\overline{\beta} + \overline{c}}{(\beta_* - \overline{\beta})^2},$$

$$B = \frac{2c_*\beta_* - c'_*\beta_*^2 + c'_*\overline{\beta}^2 - 2\overline{c}\beta_*}{(\beta_* - \overline{\beta})^2}, \tag{25}$$

$$C = \frac{-2c_*\beta_*\overline{\beta} + c_*\overline{\beta}^2 + c'_*\beta_*^2\overline{\beta} - c'_*\beta_*\overline{\beta}^2 + \overline{c}\beta_*^2}{(\beta_* - \overline{\beta})^2}.$$

Using this quadratic approximation on the interval $[\beta_*,\beta]$, integral (21) can be approximately calculated as follows:

$$\int_{\beta_0}^{\beta}\frac{c}{\beta}d\beta = \frac{A}{2}(\beta^2-\beta_0^2)+B(\beta-\beta_0)+C\ln(\beta/\beta_0). \tag{26}$$

The solution of the Riemann problem is built from two waves, left and right, which separate the disturbed region from, respectively, the left and right undisturbed regions. To construct such a solution, we introduce the functions $F_L(\beta,\beta_L,u_L)$ and $F_R(\beta,\beta_R,u_R)$ defining the state behind the left and right waves separating the undisturbed state from the disturbed one, respectively:

$$F_L(\beta,\beta_L,u_L)=\begin{cases}u_L-\sqrt{\dfrac{(\beta-\beta_L)(\sigma\beta-\sigma_L\beta_L)}{\beta\beta_L}} & \text{for } \beta\ge\beta_L,\\ u_L-A_L(\beta^2-\beta_L^2)/2-B_L(\beta-\beta_L)-C_L\ln(\beta/\beta_L) & \text{for } \beta<\beta_L,\end{cases} \tag{27}$$

$$F_R(\beta,\beta_R,u_R)=\begin{cases}u_R+\sqrt{\dfrac{(\beta-\beta_R)(\sigma\beta-\sigma_R\beta_R)}{\beta\beta_R}} & \text{for } \beta\ge\beta_R,\\ u_R+A_R(\beta^2-\beta_R^2)/2+B_R(\beta-\beta_R)+C_R\ln(\beta/\beta_R) & \text{for } \beta<\beta_R,\end{cases} \tag{28}$$

where the relations for decompaction waves in (27) and (28) should be considered only for the values $\beta_{L/R}>\beta_*$. If in the undisturbed region $\beta_{L/R}\le\beta_*$, then the corresponding functions are reduced to constants, $F_{L/R}=u_{L/R}$.

The solution of the Riemann problem depends on the solution of the nonlinear equation

$$F_L(\beta,\beta_L,u_L)=F_R(\beta,\beta_R,u_R), \tag{29}$$

which determines the value of the volume fraction in the disturbed region between the right and left waves. It is easy to see that this equation, depending on the initial data, always has either one root or no solutions at all. Depending on this, various wave configurations arise in the Riemann problem, which can be divided into the following five types.

I. Configuration without a discontinuity. In this case, the decay of the initial discontinuity gives rise to a disturbed region with parameters $\beta_s>\beta_*$ and u_s, which is separated from the undisturbed initial data, respectively, by the left and right waves. These waves can be either a compaction wave or a particle decompaction wave. We denote the velocities of these waves by λ_L and λ_R.

II. Configuration with a particle-free region on the left. This configuration occurs when $\beta_L\le\beta_*$ and there is decompaction of the compressed particles to the right of the initial discontinuity with the formation of a vacuum zone without particles $u_R\le\lambda\le\lambda_{SR}$. The right boundary of the vacuum zone is Lagrangian and moves at a velocity of λ_{SR}, equal to the velocity of the particles. The right disturbed region corresponds to the decompaction wave, in which the parameters vary from the values of the undisturbed region to the values (β_{SR},u_{SR}), where $\beta_{SR}=\beta_*$. We denote the velocity of the weak discontinuity separating the disturbed right-hand region from the undisturbed one by λ_R.

III. Configuration with a particle-free region on the right. This configuration is similar to the previous one and corresponds to the situation when the decompression wave is on the left, and the vacuum region without particles is formed on the right. The decompaction wave velocity is λ_L. The speed of the particle-void interface is $\lambda_{SL}=u_{SL}$.

IV. Configuration with two decompaction waves separated by a region without particles. This situation arises during the decay of the initial discontinuity in particles compressed to supercritical values of the volume fraction, when two waves of decompaction with specific parameters are formed. In compaction waves, the parameters of the medium change in accordance with (27) and (28) from values in undisturbed zones to values corresponding to the close packing volume fraction β_*. The vacuum zone without particles is determined by the corresponding velocities in the extreme characteristics, $u_{SL}\le\lambda\le u_{SR}$.

V. Undisturbed regions separated by a region without particles. This is the simplest situation of rarefied particles, when the initial data correspond to subcritical values and the velocities satisfy the inequality $u_L<u_R$. In this case, the initial discontinuity decays without the interaction of particles; the particles

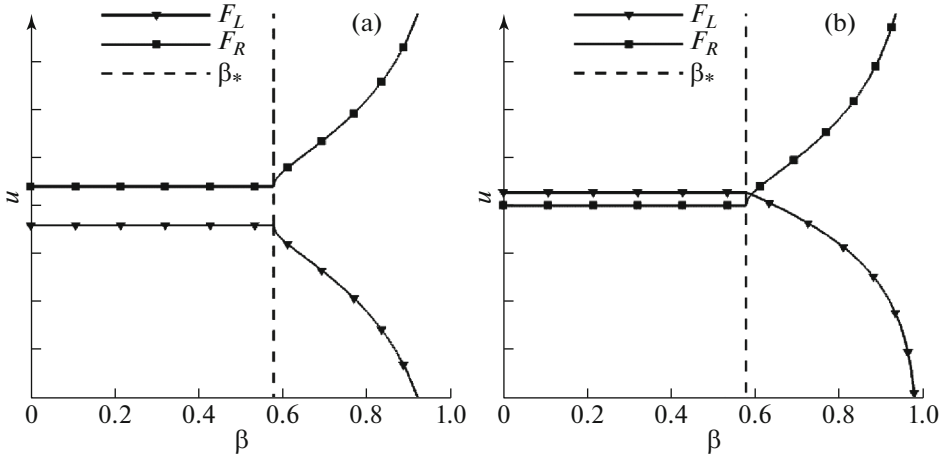

Fig. 1. Curves F_L and F_R, corresponding to the left and right waves: (a) Eq. (29) has no solution, (b) Eq. (29) has one root.

located on the left and right simply diverge due to the difference in velocities with the formation of a vacuum zone without particles.

It is easy to see that the nonlinear equation (29), which determines the solution of the Riemann problem, has no root under the initial conditions corresponding to the inequality $F_L(\beta_*,\beta_L,u_L) < F_R(\beta_*,\beta_R,u_R)$ (Fig. 1a). In this case, depending on the initial data, one of the II–V configuration types is implemented.

- Configuration II occurs if $\beta_L < \beta_*$ and $\beta_R > \beta_*$. In this case $\beta_{SR} = \beta_*$, and $u_{SR} = F_R(\beta_*,\beta_R,u_R) > u_L$.
- Configuration III occurs if $\beta_L > \beta_*$ and $\beta_R < \beta_*$. In this case $\beta_{SL} = \beta_*$, and $u_{SL} = F_L(\beta_*,\beta_L,u_L) < u_R$.
- Configuration IV occurs if $\beta_L > \beta_*$ and $\beta_R > \beta_*$. In this case $\beta_{SL} = \beta_*$ and $\beta_{SR} = \beta_*$, while $u_{SL} = F_L(\beta_*,\beta_L,u_L)$, $u_{SR} = F_R(\beta_*,\beta_R,u_R)$, and $u_{SL} < u_{SR}$.
- Configuration V is occurs if $\beta_L \le \beta_*$ and $\beta_R \le \beta_*$. If the above inequality is violated, Eq. (29) always has one root β_s (Fig. 1b). The solution of the Riemann problem in this case is of type I and consists of a two-wave configuration without a discontinuity. The particle velocity in the disturbed region is calculated as

$$u_s = F(\beta_s,\beta_L,u_L). \tag{30}$$

To solve the Riemann problem, it is required to find the root of the nonlinear equation (26). Due to the fact that the functions $F_{L/R}$ are piecewise smooth, the Newtonian iteration method is unstable. Therefore, to solve (29), a less efficient but more reliable dichotomy method was used.

The solution of the Riemann problem $\mathbf{q}^{\mathbf{R}} = \mathbf{q}^{\mathbf{R}}(\mathbf{q_L},\mathbf{q_R},\lambda)$ described above defines the numerical flow function by the standard Godunov method as the value of the differential flow on the solution of the Riemann problem: $\mathbf{\Phi}(\mathbf{z}^-,\mathbf{z}^+) = \mathbf{F}(\mathbf{q}^{\mathbf{R}}(\mathbf{z}^-,\mathbf{z}^+,\mathbf{0}))$.

4.1. Approximate Riemannian Solver Based on HLL

To simplify the calculations, we can consider an approximate solution of the Riemann problem in the same way as it is done in gas dynamics [28]. Let us describe an approximation based on the HLL approach. This approach uses the two-wave approximation. The disturbed region is characterized by a state with the average parameters $\mathbf{q}_S, \mathbf{F}_S$. The velocities of the left and right waves bounding the disturbed region will be

Table 1. Initial parameters in the problem of transporting a layer of particles

	$0 < x < 0.05$	$x > 0.05$
β	0.5	0
u, km/s	0.2	0

denoted, respectively, as D_L and D_R. Writing the Rankin–Hugoniot relations (10) for the left and right waves, we obtain

$$\mathbf{q}_S = \frac{D_R\mathbf{q}_R - D_L\mathbf{q}_L + F_L - F_R}{D_R - D_L},$$
$$\mathbf{F}_S = \frac{D_R\mathbf{F}_L - D_L\mathbf{F}_R + D_L D_R(\mathbf{q}_R - \mathbf{q}_L)}{D_R - D_L}. \tag{31}$$

By analogy with [23], we will set the value of the disturbance propagation velocity in the form

$$\tilde{\beta} = \max(\beta_L, \beta_R),$$
$$\tilde{u} = \begin{cases} (u_L\sqrt{\beta_L} + u_R\sqrt{\beta_R})/(\sqrt{\beta_L} + \sqrt{\beta_R}), & \beta_L > 0 \text{ or } \beta_R > 0 \\ 0, & \text{otherwise} \end{cases} \tag{32}$$
$$\tilde{c} = c(\tilde{\beta}),$$
$$D_L = \min(\tilde{u} - \tilde{c}, u_1 - c_1, -\varepsilon), \quad D_R = \max(\tilde{u} + \tilde{c}, u_2 + c_2, \varepsilon),$$

where $\varepsilon = 10^{-15}$. Then the corresponding value of the numerical flow in the approximate Godunov method takes the form

$$\mathbf{\Phi}_{i+1/2}(\mathbf{z}^-, \mathbf{z}^+) = \mathbf{F}_S(\mathbf{z}^-, \mathbf{z}^+). \tag{33}$$

5. CALCULATION RESULTS

The method described above was verified on a number of one-dimensional problems. In the considered problems, we used an approximation of the intergranular pressure with the parameters $\beta_* = 0.58$, $k = 0.57$, and $B/\delta = 15$, ($[B/\delta] = \text{atm/kg/m}^3$).

The first test checks the ability of the numerical method to keep particles moving at a constant velocity (the well-balancing property), and also compares the schemes of the first (the limiter in (12) is zero) and the second order of accuracy. The second test compares the numerical and analytical solutions. The third test considers the expansion of a compressed layer of particles into a vacuum. The fourth test demonstrates the effect of a gradient catastrophe of the solution and formation of a sequence of compaction waves during the passage of a compaction wave through a layer of particles with the nonuniform distribution of the volume fraction. In the fifth test, the expansion of a preliminarily compressed near-wall layer of particles is numerically studied, accompanied by the formation of characteristic structures (detachment of particles from the wall) and multiple reflections of compaction and decompaction waves from the boundaries of the layer of particles that have been detached from the wall.

5.1. Convective Transfer of a Flat Layer of Particles

We consider the motion of the particle layer with a subcritical volume fraction at a constant speed in the direction of a region without particles. The initial data of the problem is given in Table 1. The initial position of the layer boundary corresponds to $x = 0.05$ m. The calculation uses a uniform grid of 400 cells.

The calculation results are shown in Fig. 2. Here the numerical solutions at time $t = 0.1325$ are given. The layer of particles at this moment is situated in [0.265, 0.765]. Due to numerical diffusion, the boundary of the particle region is smeared on the distribution of the volume fraction. In this case, the particle velocity remains constant. The zero velocity values on the graph correspond to points with a zero volume fraction. The numerical results by the Godunov method with the exact solution of the Riemann problem and by the approximate HLL method practically coincide and, therefore, are virtually indistinguishable

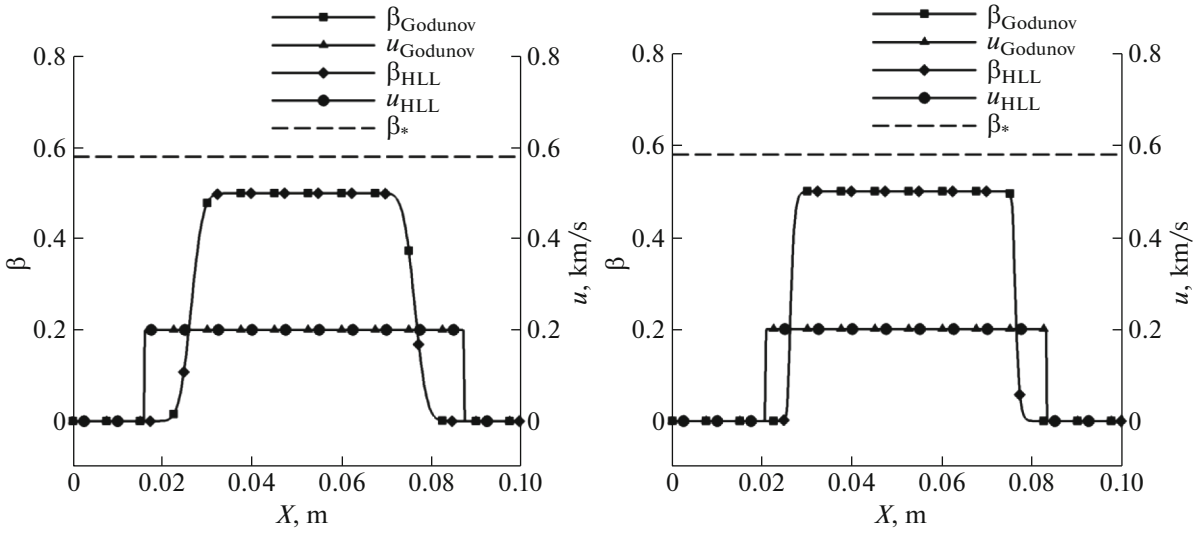

Fig. 2. Distribution of parameters in the computational domain at the moment of time $t = 0.1325$ ms; Godunov's method with exact solution of the Riemann problem and approximate HLL. The calculation according to the scheme of the first order is on the left; and the calculation according to the scheme of the second order is on the right.

on the graph. The second-order scheme gives a monotonic nonoscillating solution, which, as expected, more accurately resolves the boundaries of the particle layer with the vacuum.

5.2. Problem on the Decay of an Arbitrary Discontinuity

This test can be considered as an analog of the Sod test, which is well-known in gas dynamics. It is characterized by the presence of a shock wave and a rarefaction wave, which here are waves of compaction and decompaction of particles. The initial data for this problem is given in Table 2. It represents the initial discontinuity, which is situated at $x = 0.05$ m. To the left of the discontinuity, the particles are compressed to the supercritical value of the volume fraction; and to the right, the volume fraction corresponds to the subcritical value. A uniform grid of 400 cells was used in the calculation. The scheme of the second order was used.

Figure 3 shows the results of numerical calculations using the Godunov and HLL methods. Both methods show almost identical results. In the disturbed region, compaction occurs up to a volume fraction slightly higher than β_*. The propagation velocities of the boundaries of the decompaction wave and the compression wave are consistent with those in the analytical solution, which gives them values of -1.3878, -1.0236, and 0.3536 km/s, respectively.

5.3. Expansion of a Compressed Layer of Particles into a Vacuum

The expansion of particles with a volume fraction above the critical value into a region without particles is considered. Table 3 contains the initial data for this problem. The initial position of the boundary of the particle layer is $x = 0.05$ m. A uniform grid of 400 cells was used in the calculation.

Figure 4 presents the results of numerical calculations by the Godunov method and HLL of the second order of accuracy. In this problem, a decompaction wave propagates to the left of the discontinuity. After it, the volume fraction of the condensed phase decreases, in contrast to the previous Sod problem, exactly to the critical value β_*, and the intergranular pressure vanishes in the condensed phase. The close packing

Table 2. Initial parameters in the problem of the decay of an arbitrary discontinuity

	$x < 0.05$	$x > 0.05$
β	0.65	0.4
u, km/s	0	0

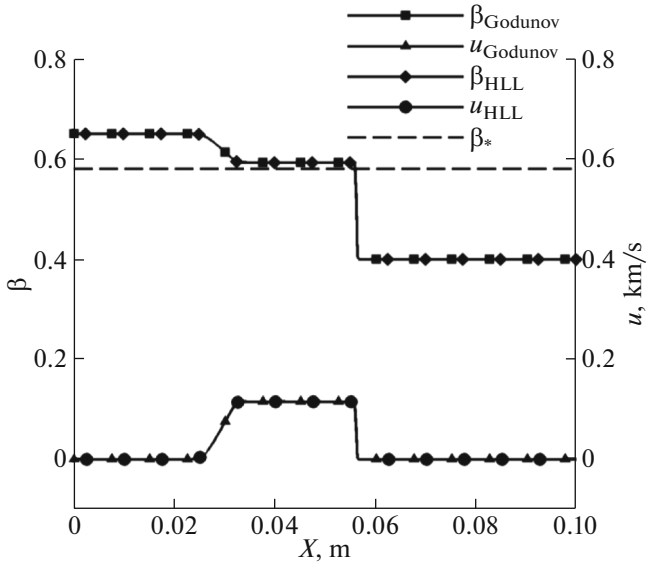

Fig. 3. Distribution of parameters in the problem of decay of the initial discontinuity at the moment of time $t = 0.0174$ ms; Godunov's method with the exact solution of the Riemann problem and approximate HLL. Scheme of the second order of accuracy.

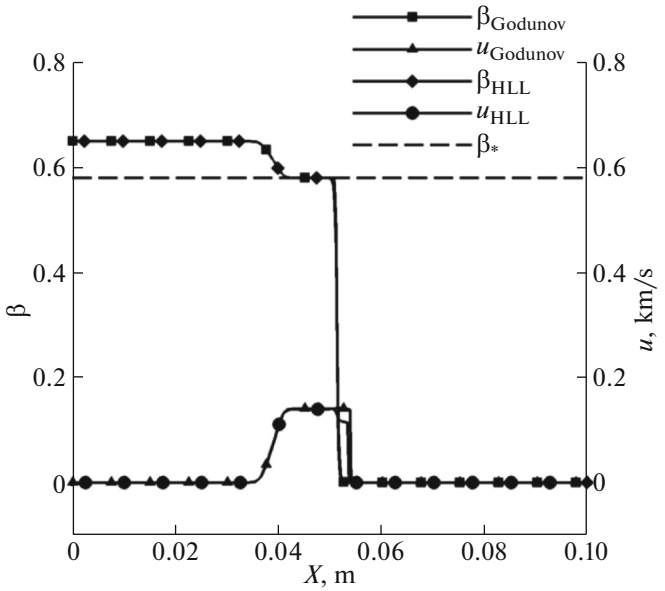

Fig. 4. Distribution of parameters in the problem of expansion into a vacuum at the moment of time $t = 0.0096$ ms; Godunov's method with the exact solution of the Riemann problem and approximate HLL. Scheme of the second order of accuracy.

interface located to the right is the Lagrangian interface that separates the region of particles from the vacuum. There is no compaction wave. The decompacted particles continue to move at a constant velocity of about 0.14 km/s. Note that in the calculation by the approximate HLL method at the interface of the con-

Table 3. Initial parameters in the problem of the expansion of a layer of particles into a vacuum

	$x < 0.05$	$x > 0.05$
β	0.65	0
u, km/s	0	0

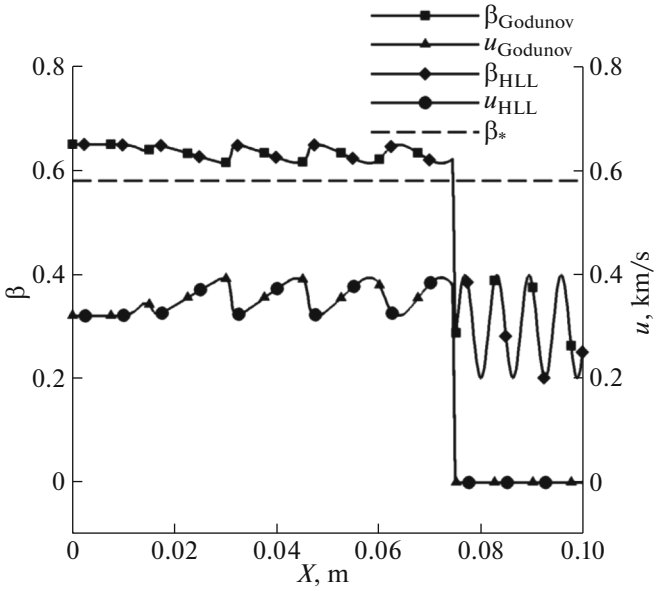

Fig. 5. Distribution of particle parameters in the wave train problem at time $t = 0.036$ ms; Godunov's method with exact solution of the Riemann problem and approximate HLL. Scheme of the second order of accuracy.

densed phase and the region without particles, the velocity of the condensed phase is described less accurately than in the Godunov scheme.

5.4. Propagation of the Compaction Wave over Inhomogeneously Distributed Particles (Wave Train)

In gas dynamics, the Shu–Osher problem [29], in which a shock wave propagates over a region with a nonuniform gas density, is well known. In the problem under consideration, the compaction wave propagates along the particle layer with a nonuniform volume fraction. Table 4 shows the initial data for this problem. The compaction wave at the initial moment is located at the point $x = 0.05$. Before the wave, the volume fraction changes according to a periodic law (second column of Table 4), when passing through which the flow parameters change from the values $\beta = 0.3$ and $u = 0$ to the values from the first column of Table 4. On the left boundary of the computational domain, the condition of the given flow rate of the condensed phase is used; and the parameters from the computational domain are interpolated on the right boundary. A uniform grid of 400 cells was used in the calculation.

Results of the numerical calculations by the Godunov and HLL methods of the second order of accuracy at the moment of time $t = 0.036$ ms are shown in Fig. 5. The compaction wave, propagating to the right, begins to interact with the unevenly distributed particles. Behind the wave front, the distribution of the velocity and volume fraction acquires a sawtooth character. The results for the Godunov and HLL schemes show identical solutions. The disturbance farthest from the initial discontinuity has a smaller amplitude, since the initial value of the volume fraction on the right corresponds to the zero value of the sine. The decreasing sections of the solution profile (compression waves) become steeper as they move away from the front of the leading compaction wave, which ultimately leads to the overturning of the fronts (the phenomenon of a gradient catastrophe) and the formation of a sequence of compaction waves moving one after another (wave train).

Table 4. Initial parameters in the analog of the Shu–Osher problem

	$x < 0.05$	$x > 0.05$
β	0.65	$0.3 + 0.1\sin(1000(x - 0.05))$
u, km/s	0.320422579	0

Table 5. Initial parameters in the problem of expansion of a near-wall layer of particles

	$x < 0.01$	$x > 0.01$
β	0.65	0.4
u, km/s	0	0

5.5. Scattering of the Near-Wall Layer of Particles

The unloading of a thin layer of particles of 0.01 m, having a volume fraction above the critical and located near a rigid wall, into a space filled with particles with a subcritical volume fraction is considered. Table 5 shows the initial parameters of the problem. The wall condition is specified on the left boundary of the region, and the first-order interpolation is specified on the right boundary. The computational domain is 0.1 m long and contains 1000 cells.

Figure 6 shows the numerical distributions for several successive moments obtained using the Godunov method and the HLL method of the second order of accuracy. Both methods show almost identical results. As a result of the decay of the discontinuity, a decompaction wave propagates along the compressed dispersed phase to the left of the discontinuity, in which the volume fraction of particles changes from the initial value to β_1, slightly above the critical level of the volume fraction (Fig. 6a). In this case, the compaction wave propagates to the right.

After reflection of the primary decompaction wave from the wall, a secondary (reflected) decompaction wave is formed, in which the volume fraction varies from β_1 to the critical value β_* (Fig. 6b). It can be seen that in the region between the secondary decompaction wave and the wall, a distribution of the medium's parameters is formed, which is characterized by a value of the volume fraction, that is constant in space and decreasing in time, and linear particle velocity profile (Fig. 6c).

To describe this structure, we consider a particular solution of Eqs. (3) of the form

$$\begin{aligned} \beta &= \beta(t), \\ u &= \alpha(t)x. \end{aligned} \tag{34}$$

It is easy to verify that such a solution exists if

$$\begin{cases} \alpha(t) = 1/(t - C_1), \\ \beta(t) = C_2/(C_1 - t), \end{cases} \tag{35}$$

where C_1 and C_2 are arbitrary integration constants.

Considering successive time moments t_1 and t_2, as well as the corresponding values of the volume fraction β_1 and β_2, the constants can be expressed as follows:

$$C_1 = (\beta_1 t_1 - \beta_2 t_2)/(\beta_1 - \beta_2), \quad C_2 = \beta_1(C_1 - t_1). \tag{36}$$

We apply the obtained solution (35) and (36) to describe the near-wall region (Fig. 6). Let us choose the time points $t_1 = 0.01573$ ms and $t_2 = 0.03005$ ms and the corresponding values of the volume fraction $\beta_1 = 0.37933$ and $\beta_2 = 0.22255$ obtained in the calculation, then the values of the coefficients are $C_1 = -0.00461$ and $C_2 = -0.00772$. Solution (34) with these values of the coefficients (Fig. 7) is consistent with the numerical solution at subsequent times as well. The time required for a decrease in the volume fraction by a factor of 100 from 0.5 to 0.005 is about 1.5257 ms, which can be considered as the particle detach time and the duration of the formation of a vacuum near-wall region.

After the interaction of the secondary decompaction wave with the primary compaction wave moving to the right along the layer of rarefied particles, a secondary compaction wave arises and begins to move in the opposite direction (Fig. 6d). Reaching the left boundary of the layer, it is reflected as a decompaction wave. Thus, the departure of a layer of particles from the wall is accompanied by a quasi-periodic wave process. It consists of a sequence of compaction waves of decreasing amplitude moving to the left, and decompaction waves moving along the layer to the right. As a result of this wave process, the momentum is redistributed, the volume fraction in the layer gradually approaches the critical value, and the layer velocity decreases. In the limit, the volume fraction in the layer reaches the critical value, and it stops at some distance from the wall.

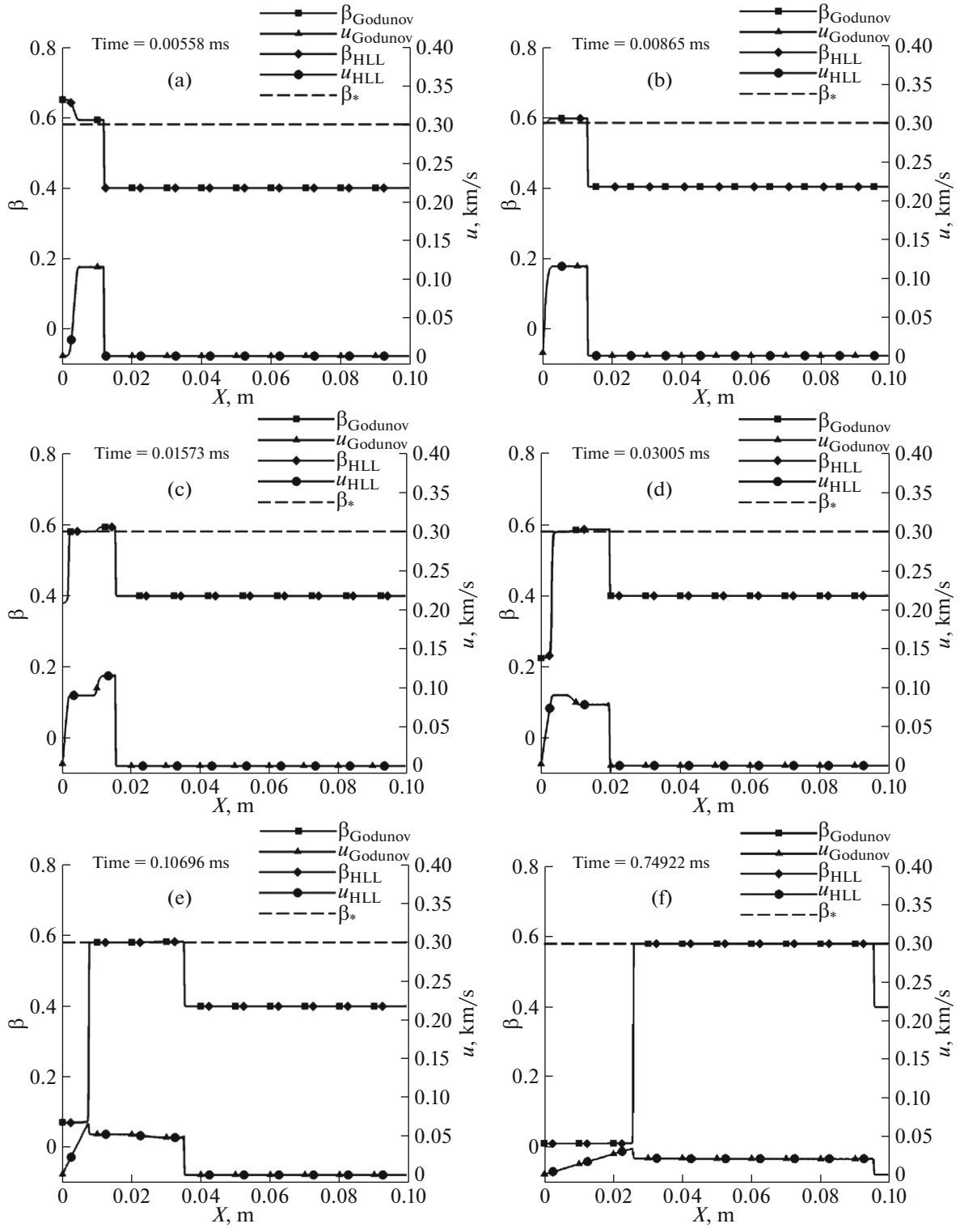

Fig. 6. Expansion of near-wall compressed layer of particles. (a) Formation of a decompaction wave; (b) beginning of reflection of a decompaction wave from the wall; (c) formation of a near-wall region of rarefied particles with a linear velocity profile; (d) compaction waves after reflection from the right boundary of the particle layer; (e) low amplitude compaction wave; (f) formation of a particle-free region near the wall.

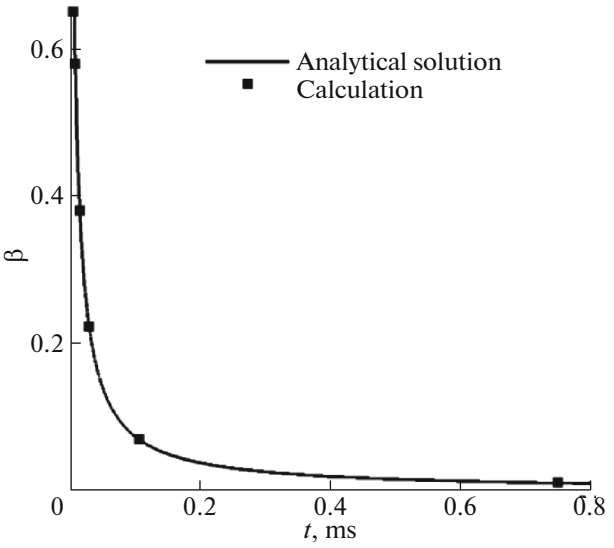

Fig. 7. Solution (34) and numerical solution at the time points corresponding to Fig. 6.

6. CONCLUSIONS

In this paper, a modification of the Godunov method is constructed based on the exact solution of the Riemann problem and the approximate HLL solution for a simplified continuum model of the motion of an ensemble of solid particles. The proposed numerical method takes into account at a discrete level the features of the system of constitutive equations of the model, which consist of the presence of a discontinuity in the propagation velocity of weak disturbances in the particle phase at the critical value of the volume fraction and the possibility of forming vacuum regions without particles.

The proposed numerical method is verified on a series of problems that admit exact solutions or their analytical estimates. The results of test calculations showed good agreement with the exact analytical solutions for quantitative wave characteristics (amplitude, wave, and characteristics propagation velocity).

Comparison of the numerical results by the Godunov method with the exact solution of the Riemann problem and the approximate HLL method showed, on the whole, almost complete agreement in all the studied test problems. A slight difference was observed in the problem of the expansion of a compressed layer of particles in the velocity profile near the particle-vacuum interface. This seems to be due to the less accurate description of the disturbance propagation velocities in the HLL method compared to the Godunov method based on the exact solution of the Riemann problem.

In the problem of propagation of a compaction wave over a layer of particles with an uneven distribution of the volume fraction, the effect of compression waves overturning behind the wave front (the phenomenon of a gradient catastrophe) and the formation of a wave train was numerically obtained.

The expansion of a near-wall layer of particles preliminarily compressed to supercritical values was studied. Quantitative characteristics were obtained and a description of the mechanism of detachment of a layer of particles from wall with the formation of a near-wall particle-free zone was proposed.

FUNDING

This study was carried out as part of a state task of the Scientific Research Institute of System Analysis, Russian Academy of Sciences on topic no. FNEF-2022-0005 (registration no. 1021060708369-1-1.2.1). The work of the first author was funded by RFBR according to the research project no. 20-31-90027.

Igor Menshov's work was supported by a state assignment of Keldysh Institute of Applied Mathematics, Russian Academy of Sciences (topic no. FFMN-2022-0002).

CONFLICT OF INTEREST

The authors declare that they have no conflicts of interest.

REFERENCES

1. Yu. P. Khomenko, A. N. Ishchenko, and V. Z. Kasimov, *Mathematical Modeling of Intraballistic Processes in Barrel Systems* (Sib. Otd. Ross. Akad. Nauk, Novosibirsk, 1999) [in Russian].
2. I. S. Menshov, M. Yu. Nemtsev, and I. V. Semenov, "Numerical modeling of wave processes accompanying combustion of inhomogeneously distributed composite propellant," Comput. Math. Math. Phys. **59** (9), 1528–1541 (2019). https://doi.org/10.1134/S0965542519090148
3. B. C. Fan, Z. H. Chen, X. H. Jiang, and H. Z. Li, "Interaction of a shock wave with a loose dusty bulk layer," Shock Waves **16** (3), 179–187 (2007). https://doi.org/10.1007/s00193-006-0059-5
4. M. R. Baer and J. W. Nunziato, "A two-phase mixture theory for the deflagration-to-detonation transition (DDT) in reactive granular materials," Int. J. Multiphase Flow **12** (6), 861–889 (1986). https://doi.org/10.1016/0301-9322(86)90033-9
5. R. I. Nigmatulin, *Dynamics of Multiphase Media*, Vol. 2 (Nauka, Moscow, 1987; Hemisphere, New York, 1991).
6. R. Saurel and R. Abgrall, "A multiphase Godunov method for compressible multifluid and multiphase flows," J. Comput. Phys. **150** (2), 425–467 (1999). https://doi.org/10.1006/jcph.1999.6187
7. R. W. Houim and E. S. Oran, "A multiphase model for compressible granular–gaseous flows: formulation and initial tests," J. Fluid Mech. **789**, 166–220 (2016). https://doi.org/10.1017/jfm.2015.728
8. T. P. McGrath II, J. G. St. Clair, and S. Balachandar, "A compressible two-phase model for dispersed particle flows with application from dense to dilute regimes," J. Appl. Phys. **119** (17), 174903 (2016). https://doi.org/10.1063/1.4948301
9. R. Saurel, A. Chinnayya, and Q. Carmouze, "Modelling compressible dense and dilute two-phase flows," Phys. Fluids **29** (6), 063301 (2017). https://doi.org/10.1063/1.4985289
10. A. N. Kraiko and L. E. Sternin, "Theory of flows of a two-velocity continuous medium containing solid or liquid particles," J. Appl. Math. Mech. **29** (3), 482–496 (1965). https://doi.org/10.1016/0021-8928(65)90059-6
11. A. N. Kraiko, "On correctness of the Cauchy problem for a two-fluid model of a gas flow containing particles," J. Appl. Math. Mech. **46** (3), 327–333 (1982). https://doi.org/10.1016/0021-8928(82)90107-1
12. A. N. Kraiko, "The mathematical models for description of flow of gas and foreign partpcles and for non-stationary filtration of liquids and gas in porous medium," Vestn. Yuzhno-Ural. Gos. Univ. Ser. Mat. Model. Program. **7** (1), 34–48 (2014). https://doi.org/10.14529/mmp140104
13. A. N. Osiptsov, "Investigation of regions of unbounded growth of the particle concentration in disperse flows," Fluid Dyn. **19** (3), 378–385 (1984). https://doi.org/10.1007/BF01093900
14. A. N. Osiptsov, "Motion of a dusty gas at the entrance to a flat channel and a circular pipe," Fluid Dyn. **23** (6), 867–874 (1988). https://doi.org/10.1007/BF01051821
15. Yu. G. Rykov, "Solutions with substance decay in pressureless gas dynamics systems," Math. Notes **108** (3), 465–468 (2020). https://doi.org/10.1134/S0001434620090187
16. N. V. Klyushnev and Yu. G. Rykov, "Non-conventional and conventional solutions for one-dimensional pressureless gas," Lobachevskii J. Math. **42** (11), 2615–2625 (2021). https://doi.org/10.1134/S1995080221110159
17. R. Saurel, N. Favrie, et al., "Modelling dynamic and irreversible powder compaction," J. Fluid Mech. **664**, 348–396 (2010). https://doi.org/10.1017/S0022112010003794
18. D. Rochette, S. Clain, and W. Bussière, "Unsteady compressible flow in ducts with varying cross-section: Comparison between the nonconservative Euler system and the axisymmetric flow model," Comput. Fluids **53**, 53–78 (2012). https://doi.org/10.1016/j.compfluid.2011.09.004
19. S. Clain and D. Rochette, "First- and second-order finite volume methods for the one-dimensional nonconservative Euler system," J. Comput. Phys. **228** (22), 8214–8248 (2009). https://doi.org/10.1016/j.jcp.2009.07.038
20. I. S. Menshov, "Exact and approximate Riemann solvers for compressible two-phase flows," Math. Models Comput. Simul. **9** (4), 405–422 (2017). https://doi.org/10.1134/S2070048217040093

21. P. G. LeFloch, *Hyperbolic Systems of Conservation Laws*: *The Theory of Classical and Nonclassical Shock Waves* (Birkhäuser, Basel, 2002).
https://doi.org/10.1007/978-3-0348-8150-0
22. A. Serezhkin and I. Menshov, "On solving the Riemann problem for non-conservative hyperbolic systems of partial differential equations," Comput. Fluids **210**, 104675 (2020).
https://doi.org/10.1016/j.compfluid.2020.104675
23. B. Einfeldt, C. D. Munz, P.L. Roe, and B. Sjögreen, "On Godunov-type methods near low densities," J. Comput. Phys. **92** (2), 273–295 (1991).
https://doi.org/10.1016/0021-9991(91)90211-3
24. B. van Leer and H. Nishikawa, "Towards the ultimate understanding of MUSCL: Pitfalls in achieving third-order accuracy," J. Comput. Phys. **446**, 110640 (2021).
25. G. D. van Albada, B. van Leer, and W. W. Roberts Jr., "A comparative study of computational methods in cosmic gas dynamics," Astron. Astrophys. **108** (1), 76–84 (1982).
26. A. V. Rodionov, "Monotonic scheme of the second order of approximation for the continuous calculation of non-equilibrium flows," USSR Comput. Math. Math. Phys. **27** (2), 175–180 (1987).
https://doi.org/10.1016/0041-5553(87)90174-1
27. P. D. Lax, *Hyperbolic Systems of Conservation Laws and The Mathematical Theory of Shock Waves* (Soc. Ind. Appl. Math., Philadelphia, 1973).
28. E. F. Toro, *Riemann Solvers and Numerical Methods for Fluid Dynamics*: *A Practical Introduction* (Springer, Berlin, 2013).
https://doi.org/10.1007/b79761
29. C.-W. Shu and S. Osher, "Efficient implementation of essentially non-oscillatory shock-capturing schemes, II," in *Upwind and High-Resolution Schemes*, Ed. by M. Y. Hussaini, B. van Leer, and J. Van Rosendale (Springer, Berlin, 1989), pp. 328–374.
https://doi.org/10.1007/978-3-642-60543-7_14